ADVANCED FUNCTIONAL MATERIALS
www.afm-journal.de

Materials Views
www.MaterialsViews.com

FULL PAPER

# Core/Shell and Hollow Ultra High Molecular Weight Polyethylene Nanofibers and Nanoporous Polyethylene Prepared by Mesoscopic Shape Replication Catalysis

*Georg F. J. Müller, Markus Stürzel, and Rolf Mülhaupt**

**Polyvinyl alcohol (PVA) nanofibers, produced by electrospinning, represent attractive high-surface-area supports for olefin polymerization catalysts. Tethered with metal alkyls, PVA nanofibers immobilize a great variety of transition metal compounds, thus producing highly active nanofiber-supported Ziegler-, metallocene-, and post-metallocene catalysts. Whereas most conventional heterogeneous polymerization catalysts form particles, PVA-nanofiber-supported catalysts enable polyolefin nanofiber and nanostructure formation by mesoscopic shape replication using electrospun nanofibers as templates. At low ethylene pressure, linear correlation between average PE/PVA core/shell fiber diameter and polymerization time are made. At elevated pressure, this control is lost, accounting for the formation of reactor blends consisting of PE granules and built-in PE/PVA nanofibers. Whereas conventional catalysts produce micrometer-sized particles of ultrahigh molecular weight PE (UHMWPE), PVA-nanofiber supported chromium catalysts afford new families UHMWPE materials. They range from UHMWPE/PVA core/shell nanofibers and nonwovens to hollow UHMWPE fibers and nanoporous UHMWPE, obtained by removing the PVA component.**

## 1. Introduction

Shape replication plays an essential role in nature and also in industrial fabrication, and surface engineering of micro- and nanometer-scaled structures.[1] For the past two decades, mesoscopic shape replication has been employed using self-assembled surfactants, polymer amphiphiles and polymer micro emulsions as templates to tailor nano-, meso- and macroporous inorganic materials, among them zeolite.[2] The engineering of compartmentalized support materials with very high surface area represents the key to effective immobilization of molecular "single-site" catalysts used in a wide variety of catalytic reactions and catalytic cascade reactions.[3] Since two decades, the major focus of catalyst research is placed upon catalyst-mediated macroscopic shape replication producing pellet-sized polyolefin granules in the reactor. The crucial point of this reactor granule technology is the controlled fragmentation of spherical mesoporous silica supported single-site catalysts during olefin polymerization.[4] Today, extending well beyond macroscopic morphology control, the attractive potential of mesoporous single-site catalysts is recognized with respect to its nano- and mesoscopic shape replication capability and production of nanostructured polyolefins. This includes the in-situ formation of polyolefin nanocrystals, nanofibers and nanopores. Yet, little is known about catalytic shape-replication processes that produce polyolefin nanofibers and highly anisotropic nanoparticles. Our approach presented herein offers great promise, because nanostructures and nanoparticles are produced in-situ, thereby eliminating significant safety hazards. It should be noted that there is a very limited synthetic access to polyolefin nanofibers as well as nanofoams. Solution based processes for nanofiber formation such as surface patterning, crystallization and orientation of polyethylene (PE) solutions in alumina nanopores[5] as well as electrospinning of PE solutions[6] offer rather limited prospects for integration into commercial olefin polymerization. Few attempts towards in-situ PE fiber formation have been made. Aida et al.[7] reported on the so-called extrusion polymerization, in which the catalyst was immobilized in the mesoporous structure of silica and growth of polyethylene occurred exclusively inside the confined environment of the channel-like cylindrical nanopores of zeolite. The single nanofibers exhibited diameters between 80 and 200 nm, depending on the deployed pore size, and aggregate to form microfibers.[8] All extrusion polymerization reactions inside such pores are rather slow and produce PE with high inorganic content, owing to the low PE yields associated with the severe plugging of the pores in the absence of catalyst fragmentation. A large number of anisotropic nanofillers such as multi-walled carbon nanotubes[9] and silica fibers[10] have been added during olefin polymerization in order to produce polyolefin nanocomposites and to improve nanoparticle dispersions by this polymerization filling technique. For example, PE nanofibers (80–130 nm) were formed on the surface of multi-walled carbon nanotubes, used as support for $Cp_2ZrCl_2$ at low temperatures.[11] This indicates that tubular pore architectures are not the prerequisite for the in-situ nanofiber formation. Similar observations were reported by Pakkanen et al.[12] who investigated ethylene polymerization on

G. F. J. Müller, M. Stürzel, Prof. R. Mülhaupt
Freiburg Materials Research Center
FMF, and Institute for Macromolecular Chemistry
Albert-Ludwigs-University of Freiburg
Stefan-Meier-Strasse 31, D-79104, Freiburg, Germany
E-mail: rolfmuelhaupt@web.de

DOI: 10.1002/adfm.201303465

zirconocene-supported mesoporous alumina with a very small pore size of only 4.3 to 7.8 nm. Moreover, Coates and Bellan attempted polyolefin nanofiber formation by means of reactive electrospinning, in which catalytic dicyclopentadiene polymerization took place during electrospinning.[13] However, this process is restricted to liquid monomers and rather difficult to control, most likely because the viscosity build-up during polymerization impairs electrospinning of nanofibers. According to Wang and Huo, silica-supported metallocene catalysts with very small rectangular pores break up in sheet fragments during polymerization, thus enabling nanosheet-like polyethylene formation by mesoscopic shape replication.[14]

In our research, we have established a versatile synthetic route to a new class of shape-replication catalysts that produce polyolefin nanofibers and a variety of nanostructured polyolefin reactor blends as well as nanoporous polyolefins. Here, main group metal alkyl-tethered polyvinyl alcohol (PVA) nanofibers and PVA nanofiber nonwovens serve as high-surface-area supports for a great variety of transition metal compounds such as titanium tetrachloride, (post-)metallocenes and half-sandwich complexes. Electrospinning of aqueous PVA solutions is well known to produce PVA nanofibers and nonwovens useful as wound dressing materials, and even as scaffolds for tissue engineering.[15] However, in order to qualify for applications in separation technology, it is imperative to render filter materials solvent resistant.[16] Therefore, another objective of this research has been to encapsulate PVA nanofibers in a shell of highly insoluble ultrahigh molecular weight polyethylene (UHMWPE).

## 2. Results and Discussion

PVA nanofibers with an average diameter of 200 ± 50 nm (cf. **Figure 1**a) were prepared by electrospinning of aqueous PVA solutions (number average molecular mass of 16 000 g mol$^{-1}$ and 17 wt% PVA content, c.f. **Scheme 1**), following procedures reported by Yarin et al.[20]

Similar to the synthesis of MAO/silica supported single-site catalysts, reported by Welborn[21] and Takahashi,[22] electrospun PVA nanofibers nonwovens were suspended in toluene, tethered with MAO, washed and used as support for (post-) metallocene and a half-sandwich chinolylcyclopentadienyl chromium (III) complex. PVA nanofibers, pretreated with AlEt$_3$ and

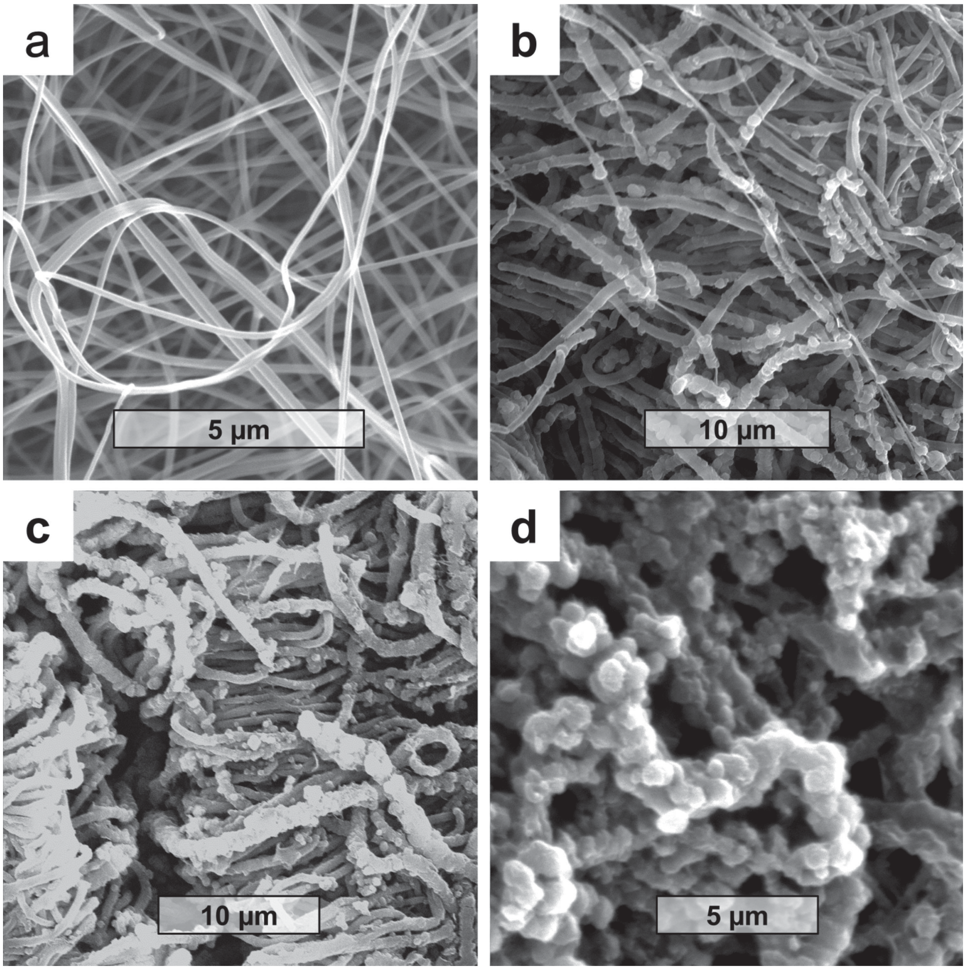

**Figure 1.** ESEM images of the electrospun PVA nanofibers (a), and PE nanofibers produced with PVA-supported Cr1/MAO (cf. Table 1) after different polymerization times of b) 6 min and c) 15 min at 0.5 bar each, and d) 5 min at 1.0 bar.

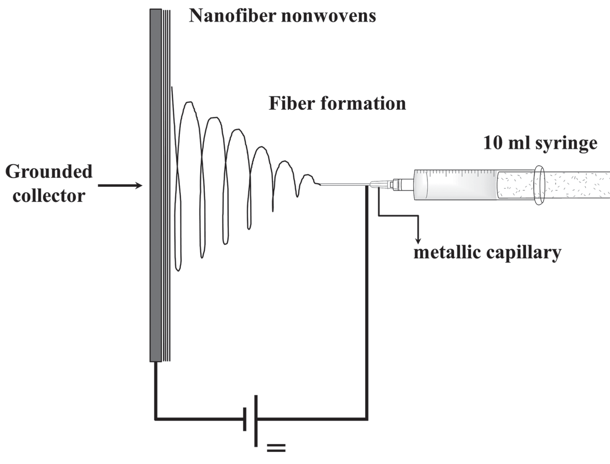

**Scheme 1.** Setup for preparing PVA nanofibers and nonwovens by electrospinning.

$MgBu_2$, were used as supports for $TiCl_4$. As is apparent from **Table 1**, all PVA-nanofiber-catalysts were active in ethylene polymerization.

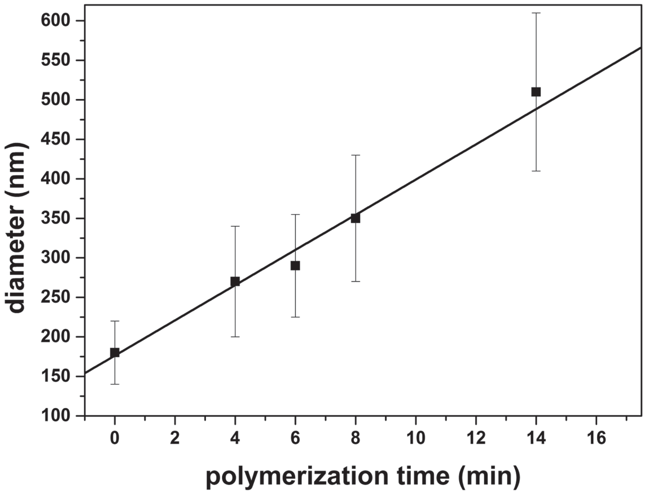

**Figure 2.** The average PE/PVA nanofiber diameter as a function of polymerization time (ethylene polymerization at low pressure of 0.5 bar).

For a more detailed analysis, ethylene was polymerized at 0.5 bar ethylene pressure and room temperature, using MAO-activated [$\eta^5$-3,4,5-trimethyl-1-(8-chinolyl)-2-trimethylsilylcyclopentadienyl] chromium (III) chloride (Cr1), supported on PVA nanofiber nonwovens. The resulting PE morphology was examined by means of Environmental Scanning Electron Microscopy (ESEM). As is apparent from Figure 1, at low ethylene pressure, PE was formed exclusively on PVA fiber surface, thus encapsulating the PVA fiber in a dense ultrathin PE shell. Clearly, the PE polymerization on PVA-fiber supported catalysts replicated the PVA nanofiber structure, thus producing PE/PVA core shell nanofibers. As the ethylene polymerization slowly progressed, the average diameter of the PE/PVA fiber shell markedly increased. In fact, as shown in **Figure 2**, the increase of average diameter of the PE/PVA core/shell nanofibers was proportional to the polymerization time. Typically, the average diameter of the PE/PVA core/shell nanofibers increased from 260 ± 70 to 500 ± 100 nm, while the PE PVA content decreased from 85 to 35 wt-% with increasing thickness of the PE shell. At higher ethylene pressures, however, this mesoscopic shape replication was lost, as indicated by the formation of spherical PE granules on top of the PE/PVA nanofibers (see Figure 1d). Hence, in a sequenced two-stage polymerization process, involving a prepolymerization at low pressures to obtain PVA/PE core/shell nanofibers, followed by ethylene pressure at elevated pressure to yield PE, reactor blends of PE/PVA nanofibers with micron-sized PE granules were produced. In contrast to the highly water-soluble PVA nanofibers, which dissolve immediately upon contact with water, even at small content of the hydrophobic PE was sufficient to render the PVA/PE core/shell nanofibers highly water insoluble. Obviously, the mesoscopic shape replication enables efficient encapsulation of PVA in a highly hydrophobic PE shell. As a consequence, water-resistant PVA/PE nanofibers and nonwovens meet the demands of separation technologies for robust nonwovens insoluble in most common solvents at room temperature.

**Table 1.** Ethylene polymerization on PVA-nanofiber-supported catalysts.[a]

| Sample | Cat.[b]/Cocat. | $p_{ethylene}$ [bar] | [µmol] | $t_{Pol}$ [min] | Activity [kg mol$^{-1}$ h$^{-1}$] | $Tm1$[c] [°C] | $Tm2$[d] [°C] |
|---|---|---|---|---|---|---|---|
| PVA/PE01 | Cr1/MAO | 1 | 1.0 | 5 | 510 | 143.6 | 136.4 |
| PVA/PE02[e] | Cr1/MAO | 0.5 | 1.0 | 4 | 214 | – | – |
| PVA/PE03[e] | Cr1/MAO | 0.5 | 1.0 | 6 | 357 | 141.1 | 137.6 |
| PVA/PE04[e] | Cr1/MAO | 0.5 | 1.0 | 8 | 750 | 141.4 | 137.6 |
| PVA/PE05[e] | Cr1/MAO | 0.5 | 1.0 | 15 | 514 | 140.1 | 140.1 |
| PVA/PE06 | Cr1/MAO | 3 | 1.0 | 120 | 1000 | 144.7 | 135.9 |
| PVA/PE07 | Ti1/MAO | 3 | 0.4 | 60 | 270 | - | - |
| PVA/PE08 | Zr1/MAO | 3 | 1.0 | 60 | 1200 | 136.4 | 130.7 |
| PVA/PE09 | Zr2/MAO | 3 | 0.7 | 60 | 640 | 138.3 | 139.1 |
| PVA/PE10 | $TiCl_4/AlEt_3$ | 3 | n.d. | 60 | 470 | 131.4 | 132.3 |
| PVA/PE11 | $TiCl_4/MgBu_2$ | 3 | n.d. | 60 | 960 | 139.1 | 137.2 |
| PVA/PE12[e,f] | Cr1/MAO | 0.5 | 1.0 | 5 | – | – | – |

[a]Reaction conditions: 25 °C, m (PVA nanofibers) = 50 mg, solvent: n-heptane = 50 mL. MAO = 800 µmol, TiBAl = 0.5 mmol; [b]Cr1 = (($\eta^5$-3,4,5-trimethyl-1-(8-chinolyl)-2-trimethylsilylcyclopentadienyl)chromium(III) dichloride; Ti1 = Bis-(*N*-(5′-tert-Butylsalicylidene)-2,3,4,5,6-pentafluoroaniline)-titanium(IV) dichloride; Zr1 = Bis-(Cyclopentadienyl)-zirconium(IV) dichloride; Zr2 = Bis-(Pentamethylcyclopentadienyl)-zirconium(IV) dichloride; [c]First heating cycle in DSC; [d]Second heating cycle in DSC; [e]Polymerization carried out in a schlenk tube with 30 mL of n-heptane; [f]Polymerization on aluminium foil exclusively for TEM thin sections.

At low ethylene pressure on PVA-nanofiber supported Cr-1, very short polymerization times, lasting only 5 minutes, enabled the recovery and analysis of single PE/PVA nanofibers with high PVA content. At high PVA content it was possible to extract PVA with water. The resulting polyethylene has ultrahigh molar mass of around $10^6$ g/mol. According to the Transmission Electron Microscopy (TEM) image, displayed in **Figure 3**, hollow UHMWPE nanofibers were formed after removal of the PVA nanofiber core. This again proofs the successful replication of PVA nanofibers and the formation of a core/shell

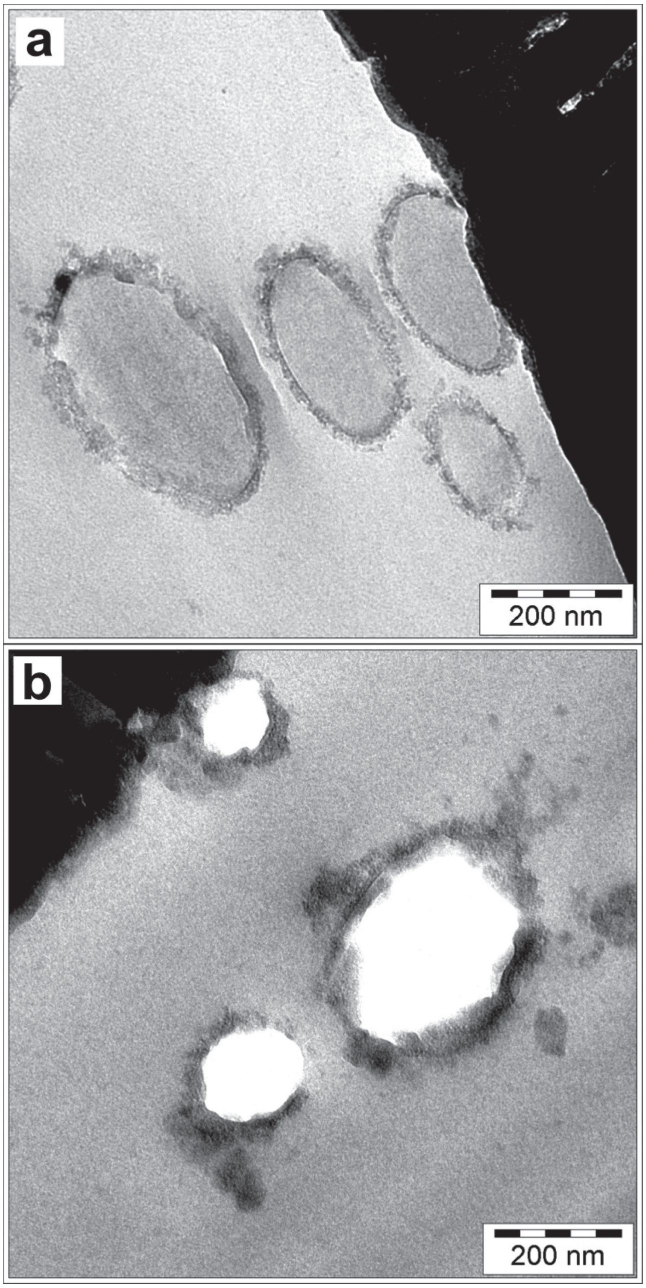

**Figure 3.** TEM image of the PE/PVA core/shell nanofibers (above) and hollow UHMWPE nanofibers after extraction of PVA with water (below). (Sample PVA/PE12; 0.5 bar ethylene pressure, polymerization time of 5 min), ultrathin sections were prepared from PE/PVA nanofibers embedded in epoxy resin).

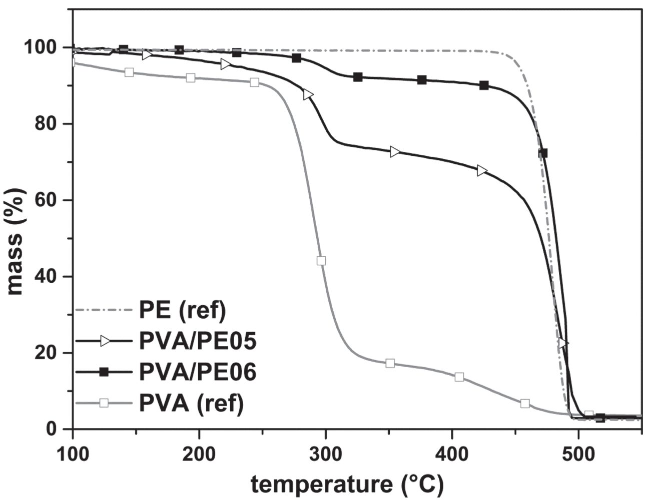

**Figure 4.** TGA-measurement of PVA/PE 06 (polymerization time of 120 min, ethylene pressure of 3 bar), PVA/PE05 (15 min, 0.5 bar) in comparison to neat PVA. The measurements were performed in a nitrogen atmosphere.

topology. It should be noted that such PE and UHMWPE nanofibers are not available by conventional processing. Moreover, the PVA nanofibers serve as templates for nanopore formation, obtained by means of PVA extraction or PVA thermal degradation, respectively. Polyolefins containing small amounts of well dispersed isolated nano-and micron-scaled pores offer potential for applications as membrane materials.[23] As a function of the PVA/PE nanofiber content, it is possible to vary the nanopore content without affecting their diameter. Whereas PVA nanofibers are highly incompatible with PE, the corresponding PVA/PE core/shell nanofibers are readily dispersed in PE by conventional PE melt compounding.

For further determination of the PVA/PE nanofiber compositions, thermogravimetric analysis (TGA) measurements were performed under a nitrogen atmosphere. According to reference measurements, the PVA degradation starts at 250 °C, whereas the PE degradation onset is around 470 °C under inert nitrogen flow. As seen in **Figure 4**, TGA measurements enable the precise determination of the PVA content of PVA/PE nanofibers. Moreover, the degradation of PVA below 300 °C in a nitrogen atmosphere represents a very effective process for removing the PVA from PVA/PE compounds. This is an attractive route for preparing nanoporous polyolefin materials, especially nanoporous UHMWPE.

## 3. Conclusion

In conclusion, the development of PVA-nanofiber-supported catalysts expands the range of supported single-site catalysts opening up a new horizon for the controlled nanostructure formation of polyolefins by means of mesoscopic shape replication. Such shape replication catalysts and reactor blend technology enables the formation of polyolefin core/shell nanofibers and nonwovens as well as hollow polyolefin nanofibers and nanoporous polyolefins, obtained by removing the PVA nanofibers in a post-polymerization step. At low ethylene pressure, the microscopic analysis clearly confirms the formation of an ultrathin and dense PE shell around PVA nanofibers. At elevated pressures the shape replication is lost. In a two-staged polymerization process, prepolymerization at low ethylene pressure forms PVA/PE nanofibers, which are embedded in PE granules when ethylene pressure is increased in the second stage. In contrast to pure PVA nanofibers, PVA/PE nanofibers are rendered water-insoluble and hydrophobic by the formation of a dense PE shell around the PVA nanofiber core. Moreover, while PVA is not melt processable, the reactor blend serves as master batch, thus enabling compounding and incorporation of PVA nanofibers into various polyolefins. Moreover, this reactor blend technique enables the production of UHMWPE nano materials which are not available by conventional processes. On thermolysis of PVA in the absence of air, nanopores are formed. Their average diameter varies as a function of the PVA fiber diameter. Furthermore, as a function of the PVA/PE content, it is possible to increase the pore content without affecting the average pore diameter. This synthetic route to nanostructured polyolefins and unusual polyolefin reactor blends offers unique opportunities of producing nanostructured polyolefin materials ranging from functional films and moldings to solvent-resistant polyolefin filters and membranes for separation technologies and even of nanoporous polyethylene and nanofoams as insulators and polymeric electrets.

## 4. Experimental Section

*Synthesis of Electrospun PVA as Support Material*: For the synthesis of PVA nanofiber nonwovens, 50 mg PVA ($M_w$ = 16000 g mol$^{-1}$, Sigma Aldrich), after drying 30 minin vacuo, was dissolved to produce an aqueous 17 wt% PVA solution. By using a syringe pump (0.7 mL h$^{-1}$), a continuous flow of the PVA solution was assured. The voltage of 30 kV for the electrospinning process was generated by the high voltage LMC 30000-2pos generator supplied by Heinzinger. The electrospinning was started as soon as a continuous flow was reached, thus spinning PVA nanofibers on aluminum foil target. Typically the electrospinning lasted 30 min.

*Preparation of the Supported Catalysts*: For supporting of single-site catalysts on the PVA nanofibers, the dried nanofiber nonwovens (50 mg) were dispersed in dry toluene (10 mL). Then 0.6 mL of MAO (900 µmol Al) were added to the dispersion. The solution was stirred for 15 min followed by extracting the supernatant liquid. After washing twice with dry toluene, the MAO-tethered PVA nanofibers were dispersed in toluene (10 mL) and the transition metal, dissolved in 10 mL toluene, was injected to this suspension. The supernatant toluene was removed after stirring for 15 min.

For the synthesis of multi-site catalysts on PVA nanofibers (PVA/PE10 und PVA/PE11; c.f. Table 1) the PVA nanofiber nonwovens (50 mg) were suspended in toluene (10 mL). A solution of the metal alkyl in toluene (0.5 mmol, 1 M) was injected in addition. After stirring for 30 min the fibers were washed twice with 10 mL of toluene. After re-suspending the fibers in n-heptane (20 mL), $TiCl_4$ (4.5 mmol) was injected, followed by refluxing the suspension. Finally, the nanofiber-supported catalysts was washed twice with n-heptane and then transferred with n-heptane (10 mL) in the reactor.

The ethylene polymerizations at 25 °C and 0.5 bar ethylene pressure were carried out in a simple Schlenk tube. Polymerization elevated pressures, higher than 0.5 bar were performed in a 200 mL glass reactor. Prior to the catalyst injection n-heptane (50 mL) and triisobutyl aluminum (0.5 mL; 1 M) were fed into the reactor. Afterwards, the resulting PE slurry was precipitated in a five-fold excess of methanol containing a small amount of conc. HCl (0.5 mL). After stirring the PE suspension for 6 h, the PE was filtered off and washed thoroughly with methanol. The resulting powder was dried at reduced pressure (65 °C) to constant weight.

*Characterization*: Thermogravimetric analysis (TGA) was carried out using the STA 409 thermal analyzer from Netzsch, Germany under nitrogen flow of 75 mL min$^{-1}$, heating rate of 10 K min$^{-1}$ and temperature range varied from 50 °C to 650 °C. Microscopy by means of SEM was carried out using an ESEM 2020 (Electroscan). The thin sections for TEM imaging were prepared using an Ultracut (Leica) and TEM LEO EM 912 Omega (Leica). Melting points and the overall thermal behavior of the neat polymer were determined by differential scanning calorimetry using a DSC 6200 from Seiko Instruments. The polymer was heated up from ambient to 200 °C, kept at that temperature for 5 min, cooled down to –70 °C and then heated up again to 200 °C. The heating rate was kept constant at 10 K min$^{-1}$. UHMWPE was achieved if the first melting cycle showed an increased melting point of the nascent polymer of 141 °C, which is characteristic for UHMWPE[17] and Cr1/MAO based heterogeneous polymerizations.[18,19]

## Acknowledgements

The authors thank the German Federal Ministry of Education and Research (BMBF, project no. 03×2006 and 03×3565C). This work was also kindly supported by LyondellBasell Polyolefine GmbH.

Received: October 9, 2013

[1] A. Zampieri, W. Schwieger, C. Zollfrank, P. Greil, in Handbook of Biomineralization: Biomimetic and Bioinspired Chemistry, (Eds: P. Behrens, E. Baeuerlein), Wiley-VCH, Weinheim, Germany **2007**, 255–288.
[2] A. Corma, *Chem. Rev.* **1997**, *97*, 2373–2420.
[3] Molecular Heterogeneous Catalysis, (Eds: R. A. van Santen, M. Neurock), Wiley-VCH, Weinheim, Germany **2006**.
[4] Tailor-made Polymers: Via Immobilization of Alpha – Olefin Polymerization Catalysts, (Eds: J. R. Severn, J. C. Chadwick), Wiley-VCH Verlag GmbH & Co. KGaA, Weinheim, Germany **2008**.
[5] H. Wu, W. Wang, Z. Su, *Gaofenzi Xuebao* **2009**, *5*, 425–429.
[6] D. M. Rein, L. Shavit-Hadar, R. L. Khalfin, Y. Cohen, K. Shuster, E. Zussman, *J. Polym. Sci., Part B: Polym. Phys.* **2007**, *45*, 766–773.
[7] K. Kageyama, J. Tamazawa, T. Aida, *Science* **1999**, *285*, 2113–2115.
[8] Y. S. Ko, S. I. Wo, in Tailor-Made Polymers Via Immobilization of Alpha-Olefin Polymerization Catalysts, (Eds: J. R. Severn, J. C. Chadwick), Wiley-VCH, Weinheim, Germany **2008**, Ch. 10, 261–276.
[9] D. Bonduel, M. Mainil, M. Alexandre, F. Monteverde, P. Dubois, *Chem. Commun.* **2005**, *6*, 781–783.
[10] A. Zecchina, *Adv. Mater.* **2006**, *18*, 3111–3114.
[11] X. Dong, L. Wang, L. Deng, J. Li, J. Huo, *Mater. Lett.* **2007**, *61*, 14–15, 3111–3115.
[12] J. P. J. Turunen, T. Venalainen, S. Suvanto, T. T. Pakkanen, *J. Polym. Sci., Part A: Polym. Chem.* **2007**, *45*, 4002–4012.
[13] L. M. Bellan, G. W. Coates, H. G. Craighead, *Macromol. Rap. Commun.* **2006**, *27*, 511–515.
[14] X. Dong, L. Wang, J. Zhou, L. Deng, J. Huo, C. Zhang, *J. Phys. Chem. B* **2006**, *110*, 13045–13049.
[15] X. Wang, C. Drew, K. J. Senecal, J. Kumar, L. A. Samuelson, *Nano Lett.* **2002**, *2*, 1273–1275.
[16] S. J. Lee, S. G. Lee, H. Kim, W. S. Lyoo, *J. Appl. Poly. Sci.* **2007**, *106*, 3430–3434.
[17] Y. M. T. Tervoort-Engelen, P. J. Lemstra, *Polym. Commun.* **1991**, *32*, 343–345.
[18] A. Kurek, S. Mark, M. Enders, M. O. Kristen, R. Mülhaupt, *Macromol. Rapid Commun.* **2010**, *31*, 1359–1363.
[19] M. Stürzel, F. Kempe, Y. Thomann, S. Mark, M. Enders, R. Mülhaupt, *Macromolecules* **2012**, *45*, 6878–6887.
[20] A. Theron, E. Zussman, A. L. Yarin, *Nanotechnology* **2001**, *12*, 384–390.
[21] H. C. Welborn, *US Patent 4,808,561, 1989*; *Chem. Abstr.* **1987**, *106*, 157033.
[22] T. Takahashi, *US Patent 5,026,797, 1991*; *Chem. Abstr.* **1989**, *111*, 58539.
[23] D. Lovera, C. Bilbao, P. Schreier, L. Kador, H.-W. Schmidt, V. Altstädt, *Polym. Eng. Sci.* **2009**, *49*, 2430–2439.